

**DEVELOPMENT OF PHOTOCATALYST FOR CO<sub>2</sub>  
CONVERSION TO HYDROCARBON FUEL**

**KOH CHAI FONG**

**BACHELOR OF ENGINEERING TECHNOLOGY  
(ENERGY AND ENVIRONMENTAL)  
UNIVERSITI MALAYSIA PAHANG**

**DECLARATION OF THESIS AND COPYRIGHT****Author's full name** : \_\_\_\_\_**Date of birth** : \_\_\_\_\_**Title** : \_\_\_\_\_

\_\_\_\_\_

\_\_\_\_\_

**Academic Session** : \_\_\_\_\_

I declare that this thesis is classified as :

 **CONFIDENTIAL** (Contains confidential information under the Official Secret Act 1972)\*

 **RESTRICTED** (Contains restricted information as specified by the organization where research was done)\*

 **OPEN ACCESS** I agree that my thesis to be published as online open access (Full text)

I acknowledge that Universiti Malaysia Pahang reserve the right as follows:

1. The Thesis is Property of University Malaysia Pahang
2. The Library of University Malaysia Pahang has the right to make copies for the purpose of research only.
3. The Library has the right to make copies of the thesis for academic exchange.

Certified By :

\_\_\_\_\_

(Student's Signature)

\_\_\_\_\_

(Supervisor's Signature)

\_\_\_\_\_

New IC / Passport Number

\_\_\_\_\_

Name of Supervisor

Date :

Date:

**NOTES** : \* If the thesis is CONFIDENTIAL or RESTRICTED, please attach with the letter from organization with period and reasons for confidentiality or restriction.

DEVELOPEMENT OF PHOTOCATALYST FOR CO<sub>2</sub> CONVERSION TO  
HYDROCARBON FUEL

KOH CHAI FONG

Thesis submitted in fulfilment of the requirements  
for the award of the degree of  
Bachelor of Engineering Technology in Energy and Environmental

Faculty of Engineering Technology  
UNIVERSITI MALAYSIA PAHANG

DECEMBER 2017

## **STATEMENT OF AWARD FOR DEGREE**

### **1. Bachelor of Engineering Technology**

Thesis submitted in fulfilment of the requirements for the award of the degree of Bachelor of Engineering Technology in Energy and Environmental.

### **SUPERVISOR'S DECLARATION**

We hereby declare that we have checked this thesis and in our opinion, this thesis is adequate in terms of scope and quality for the award of degree of Bachelor of Engineering Technology in Energy and Environmental.

Signature:

Name of Supervisor: DR. AZRINA BINTI ADB AZIZ

Position: SENIOR LECTURER, FACULTY OF ENGINEERING TECHNOLOGY,  
UNIVERSITI MALAYSIA PAHANG

Date: DECEMBER 2017

Signature:

Name of Supervisor: MDM PUTRI SHALIZA BINTI ROSMAN

Position: LECTURER, FACULTY OF ENGINEERING TECHNOLOGY,  
UNIVERSITI MALAYSIA PAHANG

Date: DECEMBER 2017

## **STUDENT'S DECLARATION**

I hereby declare that the work in this thesis is my own except for quotations and summaries in which have been duly acknowledged. The thesis has not been accepted for any degree and is not concurrently submitted for award of other degree.

Signature:

Name: KOH CHAI FONG

ID Number: TC14013

Date: DECEMBER 2017

## ACKNOWLEDGEMENTS

This thesis is completed with kind support and helps of many individuals. I would like to give my deepest appreciation to all those who guide me and provided me any kind of assistance throughout the whole process in completing my final year project which entitle “Development of Photocatalyst for CO<sub>2</sub> Conversion to Hydrocarbon Fuel”.

First and foremost, I would like to express my gratitude to our supervisor, Dr. Azrina Abd Aziz for her greatest patient, support and encouragement in guiding us to finish our project. Her useful comments, recommendations and supervision in designing, material purchasing, fabricating and performance helps me a lot while in the process of completion of this project. Furthermore, her guidance in thesis writing and mock presentation along the period of my study in completing Development of Photocatalyst for CO<sub>2</sub> Conversion to Hydrocarbon Fuel project make my presentation flows more smooth and catching.

Besides, I also want to express my special thanks to those workshop and lab assistances, En. Joharizal, En. Shamsul Azmi, En. Azlan, En. Adib and En Khairil Anuar. They are those who helping us to build our theoretical reactor to reality throughout the whole period to finish our project. Their expertise comments and recommendations on materials provide us the best solutions to build our reactor in order to finish our project.

Next, I would like to extend my sincere appreciation to my sponsor which is supported by Ftek under Senior Design Project (SDP) 2017. This provides me necessary financial support for me and my group members in accomplishing our reactor prototype.

Lastly, I would like to give my special thanks to our group members, Chai Min Choi and Nurul Izaaz binti Azmi, those who help me to assemble the parts of reactor and gives ideas about the project. Furthermore, I would like to thank to Chai Min Choi who spend his valuable time to help me finish the reactor prototype to finish our project. Thanks to Izaaz for providing us the transportation while we need. This helps us a lot when as we can complete our reactor on time because of the completion of materials. Moreover, they both also give continuous support to me while the project is ongoing. Presence of the co-operation with the different potential and abilities among

us enable us in completion prototype, individual thesis writing and presentation of this Senior Design Project.



## ABSTRACT

Owing to the limited amount of energy sources and the recent effects of fossil fuel use on the global environment, the paradigm of energy supply is changing from one based on the use of carbon-rich rocks, peat, and liquid found in the Earth to one based on renewable sources, such as energy crops, sunlight, and wind. Several methods for reducing the carbon dioxide concentration in the atmosphere and preventing CO<sub>2</sub> emissions due to human activity have been investigated, such as investigating the sorption of CO<sub>2</sub> into new/functionalized materials; increasing the quantity of green carbon sinks (plants, phytoplankton, and algae containing chloroplasts); increasing the level of dissolved carbonate and its salts in sea water; or capturing CO<sub>2</sub> and transferring it to the bottom of the sea in a supercritical state.

Photocatalytic reduction of CO<sub>2</sub> to fuels using solar energy is an attractive option for simultaneously capturing this major greenhouse gas and solving the shortage of sustainable energy. To conquer the problem of increasing CO<sub>2</sub> in the atmosphere, a solution using TiO<sub>2</sub> to convert CO<sub>2</sub> into usable fuel are conducted. Basically, the approach centres on the concept of the large-scale re-use of CO<sub>2</sub> released by human activity to produce synthetic fuels, and how this challenging approach could assume an important role in tackling the issue of global CO<sub>2</sub> emissions. There are three main objectives of this research which are to design, synthesis and develop an efficient modified nano-based TiO<sub>2</sub> to enhance the reduction of CO<sub>2</sub> to fuel, methane (CH<sub>4</sub>) through photocatalyst, to study the material chemistry of modified Nano-based TiO<sub>2</sub> who enhance the process of the photocatalyst and to utilize the prepared photocatalyst for CO<sub>2</sub> conversion to CH<sub>4</sub> in term to reduce greenhouse effect.

The photocatalytic experiment conducted by synthesising TiO<sub>2</sub>. Addition or doping with noble metal, such as platinum (Pt), palladium (Pd), silver (Ag) and gold (Au) ions allow extending the light absorption of band gap semiconductors to the visible light. Noble metals could be introduced to the surface of TiO<sub>2</sub> by various methods such as: electrolysis, chemical reduction, UV photoreduction,  $\gamma$ -reduction deposition from colloids or adsorption of metal clusters. The characterizations are focused on optical and physical characterization. Then, the evaluation of photocatalyst process is carry out in a solid gas phase photoreactor. A tungsten – halogen lamp with

high pass UV light filter are use as the visible light source. The CO<sub>2</sub> are bubbled through the water vapour into the chamber. The result is collected and analyse for the CH<sub>4</sub> yield using gas chromatography system.

The information gained from this analysis will help to contribute towards a better understanding of the main parameters that affect the activity of photocatalysts and will ultimately lead to the optimized synthesis of more efficient photocatalytic material for the photocatalytic reduction of CO<sub>2</sub> to hydrocarbon fuels.

## **Table of Contents**

<b>DECLARATION OF THESIS AND COPYRIGHT</b>	<b>ii</b>
<b>STATEMENT OF AWARD FOR DEGREE</b>	<b>iv</b>
<b>SUPERVISOR'S DECLARATION</b>	<b>v</b>
<b>STUDENT'S DECLARATION</b>	<b>vi</b>
<b>ACKNOWLEDGEMENTS</b>	<b>vii</b>
<b>ABSTRACT</b>	<b>ix</b>
<b>LIST OF TABLES</b>	<b>xiii</b>
<b>LIST OF FIGURES</b>	<b>xiv</b>
<b>LIST OF SYMBOLS</b>	<b>xv</b>
<b>LIST OF ABBREVIATION</b>	<b>xvi</b>
<b>CHAPTER 1</b>	<b>1</b>
<b>INTRODUCTION</b>	<b>1</b>
1.1 General Information	1
1.2 Problem Statement	3
1.3 Objective	4
1.4 Significant Of Research	4
<b>CHAPTER 2</b>	<b>5</b>
<b>LITERATURE REVIEW</b>	<b>5</b>
2.1 Background on Photocatalysis	5
2.1.1 Introduction	5
2.1.2 Principle of Photocatalysis	6
2.2 Graphene oxide	7
2.3 Noble Metal	8
2.4 CO <sub>2</sub> reduction	9
2.5 Photoreactor	10
<b>CHAPTER 3</b>	<b>14</b>
<b>METHODOLOGY</b>	<b>14</b>

3.1 Material	14
3.2 Synthesis of TiO <sub>2</sub>	14
3.3 Synthesis of Ag-TiO <sub>2</sub>	15
3.4 Synthesis of RGO	15
3.5 Synthesis of RGO-Ag/TiO <sub>2</sub>	15
3.6 Characterization	16
3.7 Photocatalytic Reduction of CO <sub>2</sub>	19
<b>CHAPTER 4</b>	<b>20</b>
<b>RESULT AND DISCUSSION</b>	<b>20</b>
4.1 Characterization	20
4.2 Photocatalytic Reduction of CO <sub>2</sub>	22
4.3 Project Management	26
4.3.1 Budget and Cost Analyses	26
4.3.2 Workflow	28
<b>CHAPTER 5</b>	<b>29</b>
<b>CONCLUSION AND RECOMMENDATION</b>	<b>29</b>
5.1 Conclusion	29
5.2 Recommendation	30
<b>REFERENCES</b>	<b>31</b>
<b>APPENDICES</b>	<b>33</b>

**LIST OF TABLES**

<b>Table No.</b>	<b>Title</b>	<b>Page</b>
2.1	Advantages and Disadvantages of Photoreactor Systems.	12
4.1	Budget and Cost Analyses	26
4.2	List of Cost Materials of Reactor	27
4.3	Project Workflow	28

## LIST OF FIGURES

<b>Figure No.</b>	<b>Title</b>	<b>Page</b>
2.1	Principle of Photocatalysis	6
2.2	Schematic of (A) slurry reactor design with top illumination, (B) optical fiber reactor design with side illumination and (C) internally illuminated reactor with top illumination.	11
3.1	X-ray Diffraction (XRD) machine model Burker D8 Advance	16
3.2	Field Emission Scanning Electron Microscope (FESEM) model JSM-7800F	17
3.3	UV Visible spectrometer model UV-2600, Shimadzu	17
3.4	Gas Chromatography in Central Lab	18
3.5	Schematic diagram of solid gas phase photoreactor	19
4.1	Physical surface structural of the (a) and (b) RGO-Ag/TiO <sub>2</sub> and (c) and (d) TEM images of RGO- RGO-Ag/TiO <sub>2</sub>	20
4.2	Diffraction patterns of (a) GO, (b) TiO <sub>2</sub> , (c) RGO-TiO <sub>2</sub> and (d) RGO-Ag/TiO <sub>2</sub>	21
4.3	The diagram shows (A) UV visible absorption spectra (B) Calculated bandgap energies of (a) TiO <sub>2</sub> , (b) RGO-TiO <sub>2</sub> and (c) RGO-Ag/TiO <sub>2</sub> .	22
4.4	The total yield of CH <sub>4</sub> over Control 1, Control 2, Control 3, Control 4, Anatase TiO <sub>2</sub> , RGO-TiO <sub>2</sub> , Ag-TiO <sub>2</sub> and RGO-Ag/TiO <sub>2</sub> .	23
4.5	Time dependence on the production rate of CH <sub>4</sub>	23

**LIST OF SYMBOLS**

$\text{Ag}^0$	Argentums colloid (silver colloid)
$\text{Ag}^+$	Argentums ion (silver ion)
Å	Armstrong
cm	Centimeter
°C	Degree Celsius
$e^-$	Electron
g	Gram
$\text{H}^+$	Hydrogen ion
kPa	Kilopascal
kV	Kilovolt
L	Liter
MPa	Megapascal
$\text{M}^0$	Metal colloid
$\text{M}^+$	Metal ion
m	Meter
$\mu\text{g}$	Micro gram
$\mu\text{l}$	Micro Liter
$\mu\text{m}$	Micro meter
ml	Milliliter
mm	Millimeter
min	Minute

**LIST OF ABBREVIATION**

ATP	Adenosine-5'-triphosphate
ANOVA	Analysis of variance
B-B	Box-Behnken
s-CNC	Cellulose nanocrystals
CCD	Central Composite Design
CFU	Colony Forming Unit
DNA	Deoxyribonucleic acid
EDX	Energy dispersive X-ray spectrometer
EPA	Environment Protection Authority
EC	Epicatechin
ECG	Epicatechin-3-gallate
EGC	Epigallocatechin
EGCG	Epigallocatechin-3-gallate
E. coli	Escherichia coli
FESEM	Field emission scanning microscope
FDA	Food and Drug Administration
FTIR	Fourier transform infrared spectroscopy
FFD	Full Factorial Design
GC	Gallocatechin
HPMC	Hydroxypropyl methylcellulose
ICDD	International Centre for Diffraction Data
MNP	Metal nanoparticles



OFAT	One factor -at-a-time
PHB	Poly(3hydroxybutyrate)
PCL	Poly( $\epsilon$ -caprolactone)
PGA	Poly(glycolic acid)
PEG	Polyethylene glycol
PLA	Poly(lactic acid)
ROS	Reactive oxygen species
RSM	Response surface methodology
AgNP	Silver nanoparticles
SNP	Silver nanoparticles
AgNO <sub>3</sub>	Silver nitrate
SS	Sum of squares
SPR	Surface plasmon resonance
SERS	Surface-enhanced Raman scattering scattering
TEM	Transmission electron microscopy
XRD	X-ray diffraction

## CHAPTER 1

### INTRODUCTION

#### 1.1 General Information

Global warming issue is getting crucial nowadays. This issue mainly caused due to the unstoppable increasing atmospheric carbon dioxide (CO<sub>2</sub>) which produced by human being activities. Greenhouse gases are the main factor which causes the global warming. In the composition of greenhouse gases, there is 72% of totally emitted CO<sub>2</sub>, 18% of methane (CH<sub>4</sub>) and 10 % of nitrous oxide (NO<sub>x</sub>). It is clearly stated, CO<sub>2</sub> are the most important causes of global warming. The source of production CO<sub>2</sub> is mostly by burning fuels like e.g. natural gas, dieses, organic diesel, petrol and oil. According to International Panel on Climate Change (IPCC), the atmospheric CO<sub>2</sub> level was estimated that it could reach up to 590 ppm by 2100 and the global mean temperature would rise by 1.9 °C (Li, An, Park, Majeda & Tang, 2014). The greenhouse gases will seriously impact in many different aspects, such as ice melting at the Earth's pole, fast rising sea level and increasing precipitation across the globe. CO<sub>2</sub> molecule is very stable which is not easily transformed into others chemical in a reaction. By using photocatalyst, CO<sub>2</sub> can be served as a building block for the synthesis of other useful chemicals and chemical intermediates.

The photocatalyst for the conversion of carbon dioxide (CO<sub>2</sub>) into hydrocarbon fuels with the visible light energy is a promising and eco-friendly approach to prevent the increase in greenhouse gases and exhaustion of fossil resources. Among the semiconductor materials like Titanium dioxide (TiO<sub>2</sub>), Zinc oxide (ZnO), Tungsten oxide (WO<sub>3</sub>) and Zinc Sulphide (ZnS), TiO<sub>2</sub> is one of the most promising photocatalyst due to its versatile characteristics including non-toxicity, low cost, high photocatalytic and chemical biologically inert. From the TiO<sub>2</sub> materials, TiO<sub>2</sub> nanoparticles are great interest in photocatalytic properties, hence it is used in antiseptic and antibacterial compositions. Furthermore, it is also been used in many application such as degrading organic contaminants and germs, UV-resistant material, manufacture of printing ink, self-cleaning ceramics and glass, coating. Nevertheless, TiO<sub>2</sub> nanoparticles also used in

making of cosmetic products such as sunscreen creams, whitening creams, morning and night creams, skin milks and in the paper industry for improving the opacity of paper.

However, the photocatalytic activity of  $\text{TiO}_2$  is limited by its low capability of absorption in the visible light and fast recombination rate of the photogenerated electron-hole pairs. The wide band gap (3.2 eV for anatase and 3.0 eV for rutile) of  $\text{TiO}_2$  only can be excited in UV range of spectrum ( $\lambda < 380\text{nm}$ ). It covers only  $\sim 5\%$  of the whole solar spectrum compared to the visible light spectrum (Sim, Leong, Phichiah & Shliza, 2015). Various studies have been carried out to improve the photocatalytic activity of  $\text{TiO}_2$  by doping with noble-metals and non-metals. Besides,  $\text{TiO}_2$  can be coupled with semiconductors. The noble metal such as gold (Au), silver (Ag), and copper (Cu), possess a great ability of visible light absorption due to existence of localized surface plasmon resonance (LSPR). LSPR is an optical phenomenon which is generated by light when it contacts with conductive nanoparticles (NPs) that are smaller than the incident wavelength. As in surface plasmon resonance, the electric magnetic force of incident light can be settled to collect and excite electrons of a conduction band, with the result being coherent localized plasmon oscillations with a resonant frequency that strongly depends on the composition, size, geometry, dielectric environment and separation distance of NPs (Eleonora petryayeva, Ulrich J.krull, 2011). Moreover, noble metal will transfer the electron to  $\text{TiO}_2$  and traps the electron in the metal  $\text{TiO}_2$  nanostructures to minimize the surface charge recombination in  $\text{TiO}_2$ .

Further studies have been devoted to improve the optical absorption and increase the charge carrier transport. Reduced graphene oxide (RGO) was used in the hybrids thus to diminish the bandgap and minimize the electron-hole recombination rate. Graphene is a two-dimensional  $\text{sp}^2$ -hybridized carbon nanosheet which consists of rich characteristics including high specific surface area, high electron mobility and tunable band gap. Liang et al. prove that the less deficient graphene- $\text{TiO}_2$  nanocomposite thin film resulted in larger improvement of photocatalytic activity for the photoreduction of  $\text{CO}_2$  to  $\text{CH}_4$ . Tan et al. described that graphene- $\text{TiO}_2$  nanocomposite adopted the ultraviolet light (UV) to produce a maximum  $\text{CH}_4$  product yield of  $0.135\mu\text{mol g cat}^{-1} \text{h}^{-1}$ , which is 2.1 and 5.6 fold higher than graphite oxide and pure anatase. These studies have shown that the enhancing effects of graphene on the photocatalytic activity of  $\text{TiO}_2$  in hybrid materials.

Recent years, research shows that the graphene- $\text{TiO}_2$  nanocomposite is limited to photodegradation of organic pollutants. This encourages people to do more research

toward the photocatalytic conversion of CO<sub>2</sub> to CH<sub>4</sub> with the assist of RGO as the proficient electron trapper to overwhelm the recombination of photoinduced electron-hole pairs.

## 1.2 Problem Statement

Nowadays, the issues of the CO<sub>2</sub> cause the global warming getting serious. CO<sub>2</sub> are the highest gases which contains around 72% of the greenhouse gases. This mean that CO<sub>2</sub> are the most serious causes of global warming compared to another two gases (18% of CH<sub>4</sub> and 9% of NO<sub>x</sub>). The supply of CO<sub>2</sub> is definitely comes from by burning fuels such as natural gas, diesel, organic- diesels, petrol and oil. The discharge of CO<sub>2</sub> to atmosphere have been increase overnight within the last 50 years and still increase by almost 30% each year. The CO<sub>2</sub> that released to the atmosphere will remains for 100 to 200 years. This lead the concentration of CO<sub>2</sub> in atmosphere increase, hence the earth temperature increase. The CO<sub>2</sub> gives the serious impact in different aspect such as ice melting at the Earth's pole, fast rising sea level and increasing precipitation across the globe (Li, An, Park, majeda & Tang, 2014).

Most of the photochemistry and photoelectrochemistry process involves the excitation of TiO<sub>2</sub> by photon with light energy greater than energy gap. However, the wide band gap (3.2 eV for anatase and 3.0 eV for rutile) only can excited with UV light which covers ~ 5% of the irradiation ( $\lambda < 380$  nm) from the total solar spectrum. The solar spectrum consists of ~ 43% of the visible light and the remaining ~52% is infrared light. The availability of UV spectrum is marginal in comparison to the visible light spectrum. Hence it causes a major limitation of utilizing the UV source for its natural activation. Thus the present available TiO<sub>2</sub> is not suitable for the utilization of visible spectrum of solar energy. Therefore, the employment of solar energy for a photocatalytic process can be improved by altering the energy gap response of TiO<sub>2</sub> to the visible light region (Yu, Zhang, Cheng, & Su, 2007).

### 1.3 Objective

- i. To synthesize highly pristine anatase TiO<sub>2</sub> nanoparticles (NPs) as template through a simple, facile and easy method.
- ii. To identify noble metals from the periodic table along with a novel, smart, ease and sustainable method to incorporate them onto TiO<sub>2</sub> template for activating LSPR phenomenon.
- iii. To investigate the contribution of carbon materials for visibility, electron mobilizing and charge carriers' transportation by wrapping it onto the synthesized composite photocatalysts.
- iv. To characterize the prepared nanocomposite photocatalysts for its various intrinsic natures through crystalline phase analysis, morphology, elemental composition and optical properties.
- v. To evaluate the visible light photocatalysis ability of the synthesized nanocomposite photocatalysts by converting CO<sub>2</sub> to CH<sub>4</sub>.

### 1.4 Significant Of Research

Modified nano-based TiO<sub>2</sub> has great contribution towards the environment. In treatment of waste water, TiO<sub>2</sub> nanoparticles have the great potential for removal of organic pollutant from the waste water. However, it is not very practical in the industry because of its low oxidation rate. By comparing TiO<sub>2</sub> nanoparticle conversion process with other wastewater treatment such as activated sludge reactor, membrane bioreactor and etc., TiO<sub>2</sub> nanoparticle conversion no need to undergo the treatment for the sludge of the wastewater for secondary and tertiary treatment.

To solve the CO<sub>2</sub> problem permanently, it requires transformation of CO<sub>2</sub> into another useful or non-toxic compound. In our research, we use the principle of photoconversion to conquer the problem of increasing CO<sub>2</sub> in the atmosphere. The solution by using TiO<sub>2</sub> to convert CO<sub>2</sub> into usable fuel is conducted. The TiO<sub>2</sub> photoreduction's end product does not produce any toxic gases. The final gas produce is the dominant hydrocarbon, CH<sub>4</sub>. The production of CH<sub>4</sub> will be another alternative to replace the fossil fuel in the future. Thus, by upgrading CO<sub>2</sub> to reusable hydrocarbon resources definitely would benefit humans and the environment.

## CHAPTER 2

### LITERATURE REVIEW

#### 2.1 Background on Photocatalysis

##### 2.1.1 Introduction

TiO<sub>2</sub> has been widely recognized as an excellent photocatalyst. It is known to have superb pigmentary properties, high adsorption in the ultraviolet region, and high stability which allows it to be used in various applications such as electroceramics, glass, and photocatalytic purification of chemical in air and water (Cheng Chee Kaan et al., 2012). The acceleration of a chemical transformation by the presence of a catalyst with light is called photocatalysis. The catalyst may increase the rate of photoreaction by interaction with the substrate in its ground or excited state and/or with a primary photoproduct, depending upon the mechanism of the photoreaction and itself remaining unaltered at the end of each catalytic cycle (Haque et al., 2012). There are many semiconductor materials can be used as a photocatalyst. Semiconductors like TiO<sub>2</sub>, ZnO, Fe<sub>2</sub>O<sub>3</sub>, CdS, ZnS etc. are all suitable materials to initiate a photocatalytic process (Kaan et al., 2012).

Photocatalysis, which initiates the breakdown of organic molecules into simpler aliphatic molecules and eventually to CO<sub>2</sub>. An additional mineral acids are involved in several of the natural purification of aqueous system lagoons, ponds, streams, rivers and lakes. The process is well supported by the sunlight, a natural sensitizer. In 1976, the employment of 'colloidal semiconductors' and the beginning of catalysts to promote specific redox processes on semiconductor surfaces were developed (Kalyanasundaram, 1983). Since then, naturally occurring semiconductors that could boost this solar driven purification process have been proven in laboratory scale (Matthews, 1993). Wrapping up, the solar photocatalytic process can also be applied to removal of trace metals, destruction of organics, removal of inorganic compounds, degradation of natural organic matter and medical applications (Alex Omo Ibadon and Paul Fitzpatrick, 2013).

### 2.1.2 Principle of Photocatalysis

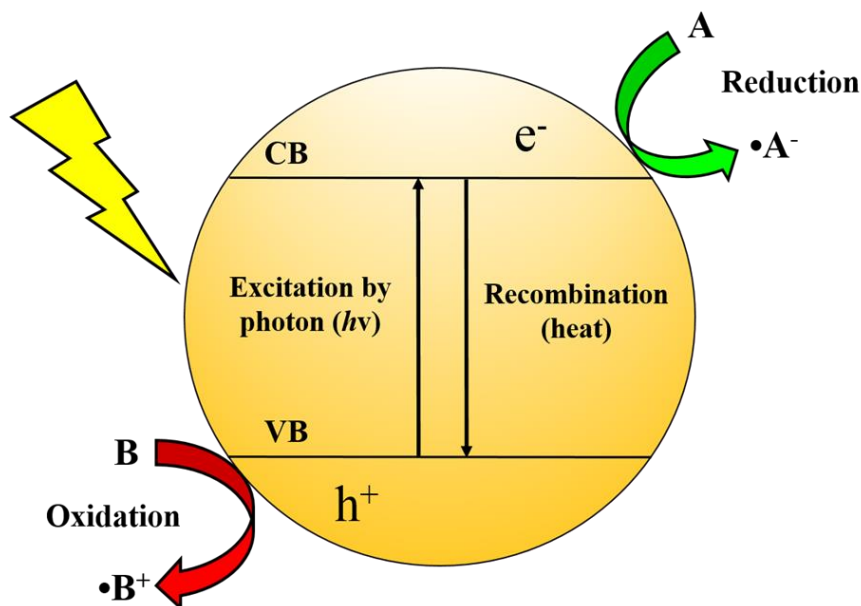


Figure 2.1: Principle of Photocatalysis

The acceleration of a chemical reaction by direct irradiation or irradiation of a catalyst that minimize the activation energy for the first reaction to occur is described as photocatalysis. Photocatalytic oxidation (PCO), which also called as heterogeneous photocatalysis, has been applying since the mid-1970s to sanitize water from harmful microorganisms. Besides, it has been applied to compensate for insufficiencies in spore destruction and decontamination in ultraviolet germicidal irradiation (UVGI) air disinfection systems (Hoffmann et al., 1995). Inertness to chemical environment and long-term photostability has made  $\text{TiO}_2$  an important material in many practical applications, and, in commercial products ranging from drugs to foods, cosmetics to catalysts, paints to pharmaceuticals, and sunscreens to solar cells in which  $\text{TiO}_2$  is used as a desiccant, brightener, or reactive mediator (Alex Omo Ibadon and Paul Fitzpatrick, 2013).

Photocatalysis processes involve the initial absorption of photons by a molecule or the substrate to produce highly reactive electronically excited states (Amy L. et al., 1995). When a photocatalyst is exposed with photons with energies greater than the semiconductor's band gap,  $E_g$  (eV), an electron is carried to the CB and leaves a positive hole in the VB. This is called an electron-hole pair (Alex Omo Ibadon and Paul Fitzpatrick, 2013). The efficiency of the photocatalytic process is measured as a

quantum yield which is defined as the number of events occurring per photon absorbed. The ability to measure the actual absorbed light is very difficult in heterogeneous systems due to scattering of light by the semiconductor surface. It is usually assumed that all the light is absorbed and the efficiency is quoted as an apparent quantum yield. If several products are formed from the photocatalytic reaction the efficiency is sometimes measured as the yield of a particular product (Amy L. et al., 1995).

The most common approach to categorize the trapping sites of electrons below the CB is purely based on their energy position in respect to CB and depicted as preexisting defect states, 5,8–10 suggestively called ‘shallow’ and ‘deep’ traps. The deep traps are consensually associated to O<sub>2</sub> defect sites, namely vacancies, which are more abundant on TiO<sub>2</sub> surface due to unsaturated coordination related to crystal termination. The shallow traps on the other hand are a matter of intense discussion and there is not to date an unambiguous structural feature associated with them that is consensual (Fabio G. Santomauro et al., 2015).

The resistance between charge-carrier recombination and charge transfer is the one that determine overall quantum efficiency for interfacial charge-carrier transfer (Hoffmann et al., 1995). The band positions or flat band potentials of the semiconductor material is also of great importance which indicates the thermodynamic limitations for the photoreactions that can take place.

## **2.2 Graphene oxide**

Graphene, which consists of a single atomic layer of sp<sup>2</sup> two-dimensional (2D) hybridized carbon atoms arranged in a honeycomb structure, is a basic building block for all graphitic forms. The initial application of graphene was in the field of electronic devices, concentrated upon its electronic properties. The studies on graphene reveal that it possesses other exciting properties, such as high stiffness and strength, excellent thermal properties and promising biocompatibility (Jianchang Li et al., 2014).

The techniques concluded for synthesizing graphene can be grouped into six major methods, i.e., mechanical cleavage, epitaxial growth, chemical vapor deposition (CVD), total organic synthesis, and chemical method. Recently, GO has gained more attention because it is functionalized easily with fluorescent probe and other compatible biomolecules (Liu, et al., 2010; Pham, et al., 2011). These unique properties of GO



make it a promising nanomaterial for bioapplication. Industrially produced GO could be used for wide range of application such as solar cell (Xinjuam, et al., 2012), hydrogen storage (Wang, et al., 2007), transparent conductive films (Park, et al., 2010), Polymer composite (Zhang, et al., 2009, Eda and Chhowalla, 2009), Paper like materials (Dikin, et al., 2007), biomedicine (Mohanty and Berry, 2008; Yousefim, et al., 2012; Bykkam, et al., 2013), fabricating nanoelectronic devices (Bunch, et al., 2007), energy storage devices (Liu, et al., 2010), biosensors (Prabhakar, et al., 2008; Lu, et al., 2009; Zhou, et al., 2010; Yancai, et al., 2013), catalysis (Chauhan, et al., 2011) and transparent electrodes (Zhang, et al., 2010).

GO also possesses nontoxological effects and hence can be widely used in medicinal research. Due to antimicrobial activity of GO, they can also be employed in dental resin composites, bone cement, ion exchange fibers and coatings for medical devices, biosensors and nano-biotechnology research. The results showed that GO nanoparticles presented good antibacterial activity effective against common human pathogenic microorganism (Bao, Qi, Dun Zhang and Peng Qi, 2011).

The fusing of graphene with  $\text{TiO}_2$  can create compound with both exceptional characters and functions of two components and lead to some additional novel properties. Thus, graphene-based photocatalyst own great numbers of chance for the photocatalytic  $\text{CO}_2$  reduction field. Due to the unique structure and excellent electronic, thermal and mechanical properties, graphene is expected to be catalyst supports. The combination of graphene with  $\text{TiO}_2$  can create composites with both the outstanding characters and functions of two components and lead to some additional novel properties. Thus, graphene-based photocatalyst possesses numerous opportunities for the photocatalytic  $\text{CO}_2$  reduction field (Liu, Jinghua, et al., 2016).

### **2.3 Noble Metal**

Metal nanoparticles are widely used to construct structures that possess unique electric, photonic and catalytic properties such LSPR, SERS and SEF (Zhang, YuJuan, et al., 2012). Nanoparticles of Ag, Au, Cu, Fe and its oxides, Pd and Pt can be utilize in catalyzing reactions, which provide immense scope for green chemistry. Fe and its oxide nanoparticles are excellent materials for environmental remediation. Nanoscale materials are used as sorbents for contaminants, in nanofiltration and in reactive

membranes. The use of metal nanoparticles in sensing could bring about a revolution in biology, healthcare, military and day-to-day life (Nair, A. Sreekumaran, et al., 2007).

In particular, the extinction spectra of noble metal nanoparticles are dominated by LSPR. These resonances are attributed to a coherent excitation of the CB electrons, excited by means of an electromagnetic field. In the presence of the oscillating electromagnetic field of the light, the free electrons of the metal nanoparticle undergo a collective coherent oscillation with respect to the positive metallic lattice (Hu, Chun, Tang, Yuchao, Jiang, Zheng, Hao, Zhengping, Tang, Hongxiao and Wong, Po Keung, 2003).

Addition or doping with noble metal, such as Pt, Pd, Ag and Au ions allow to extend the light absorption of band gap semiconductors to the visible light. Noble metals could be introduced to the surface of TiO<sub>2</sub> by various methods such as: electrolysis, chemical reduction, UV photoreduction,  $\gamma$ -reduction deposition from colloids or adsorption of metal clusters. It was proved that doping with [Pt<sub>3</sub>(CO)<sub>6</sub>]<sub>n</sub><sup>2-</sup> (n=3-10) clusters could enhance the photoconversion yield by inhibition of the electron hole recombination (Grabowska, Ewelina, Hynd Remita, and Adriana Zaleska, 2010).

The effect of the metal modification on the photocatalytic activity depends on the type of metal, metal precursor concentration used during synthesis and the origin of titania. Generally, the surface modified with Ag, Au and Pt clusters exhibits better efficiency in phenol photooxidation than TiO<sub>2</sub>-based photocatalysts. It was discovered that Ag and Pt transform titania surface to expand the photocatalytic activity both under UV and visible light irradiation (Grabowska, Ewelina, Hynd Remita, and Adriana Zaleska, 2010).

## **2.4 CO<sub>2</sub> reduction**

The past few decades have witnessed the problem of global warming, which is dominantly caused by CO<sub>2</sub> emissions from fossil fuel consumption. Therefore, seeking for any alternative to minimize CO<sub>2</sub> emission has attracted increasing attention all over the world. The traditional method used to solve this problem is carbon capture and storage, but in fact this problem has never been solved radically because CO<sub>2</sub> does not convert into other substances. The photocatalytic reduction of CO<sub>2</sub> into hydrocarbon fuels was found to be a prospective way (Liu, Jinghua, et al., 2016). The energy grade of

CO<sub>2</sub> is low from a thermodynamic perspective, accounting for why any transformation to hydrocarbon requires energy infusion. The energy source should be provided without producing more CO<sub>2</sub>, such as solar energy (Wu, Jeffrey, and Hung-Ming Lin, 2005).

Photocatalytic CO<sub>2</sub> conversion is a complicated combination of photophysical and photochemical processes. The redox reaction is initiated by photoexcitation when the energy of photons equal to or greater than the band gap of a semiconductor is received by the photocatalyst. Then the electrons are excited from the VB to the CB (Li, Kimfung, et al., 2014).

## **2.5 Photoreactor**

The important aspect that might affect the photocatalytic efficiency is the arrangement of catalyst particles in the photoreactor system. Photoreactor act as a holder where phtocatalyst, reactant and photon meet. There are two main parameters that determine the types of photoreactor for CO<sub>2</sub> photoreduction which are:

1. Phases: gas-solid, liquid-solid, gas-liquid-solid and etc.
2. Mode of operation: batch, semi-batch, continuous and etc.

Photocatalyst can normally be tested in a photoreactor configuration in suspended or fixed form as shown in Figure 2.2. An ideal photoreactor must equip with best lighting distribution into the system. Then, the comparative analysis of the yield of CO<sub>2</sub> emission reduction products and reactor configuration is mainly based on quantum efficiency. Table 1 summarizes the advantages and the disadvantages of the different types of photoreactor systems which used for CO<sub>2</sub> photoreduction (Oluwafunmilola Ola, M.Mercedes-Valer, et al., 2015).

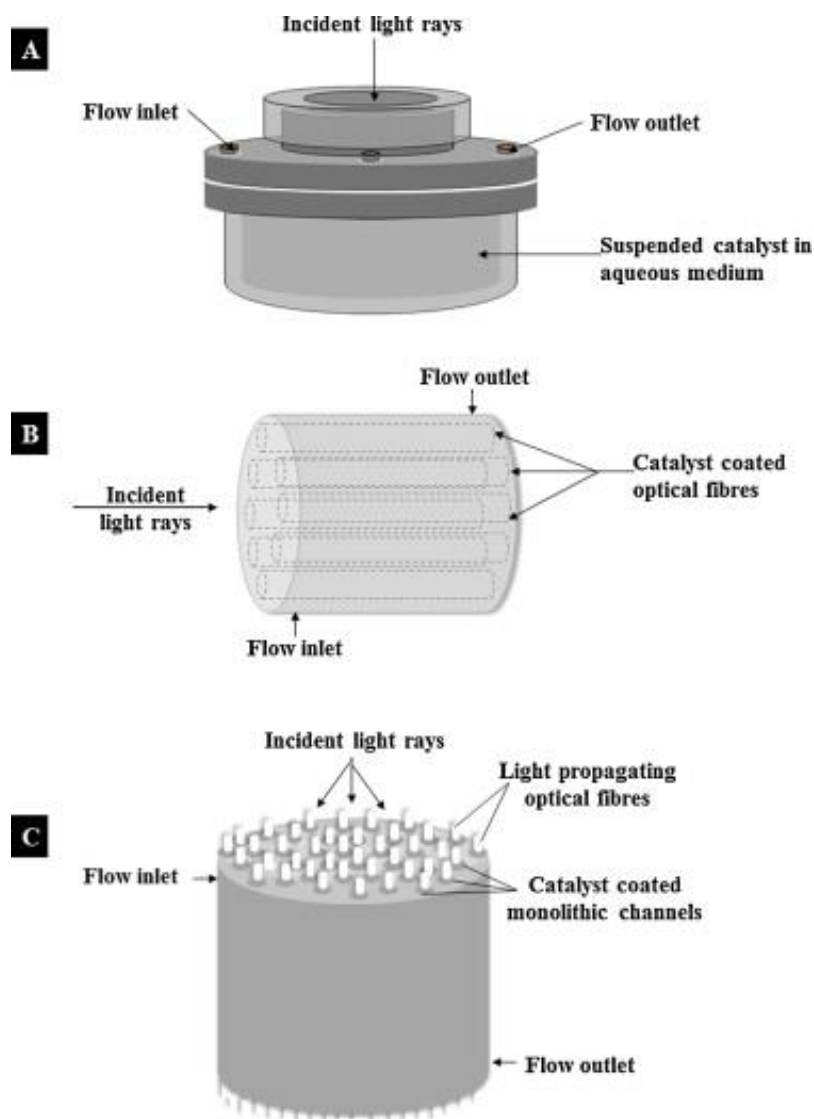


**Figure 2.2:** Schematic of (A) slurry reactor design with top illumination, (B) optical fiber reactor design with side illumination and (C) internally illuminated reactor with top illumination.

**Table 2.1:** Advantages and Disadvantages of Photoreactor Systems.

Reactor design	Advantages	Disadvantages
<b>Fluidized and slurry reactor (multiphase)</b>	<p>(I) Temperature gradients inside the beds can be reduced through vigorous movements caused by the solid passing through the fluids</p> <p>(II) Heat and mass transfer rates increase considerable due to agitated movement of solid particles</p> <p>(III) High catalyst loading</p>	<p>(I) Filters (liquid phase) and scrubbers (gas) are needed</p> <p>(II) Flooding tends to reduce the effectiveness of the catalyst</p> <p>(III) Difficulty of separating the catalyst from the reaction mixture</p> <p>(IV) Low light utilization efficiency due to absorption and scattering of the light by the reaction medium</p> <p>(V) Restricted processing capacities due to mass transport limitations</p>
<b>Fixed bed reactor</b>	<p>(I) High surface area</p> <p>(II) Fast reaction time</p> <p>(III) The conversion rate per unit mass of the catalyst is high due to the flow regime close to plug flow</p>	<p>(I) Temperature gradient between gas and solid surface is common</p>

	(IV) Low operating costs due to low pressure drop	
<b>Monolith reactor</b>	<p>(I) High surface to volume ratio and low pressure drop with high flow rate can be achieved</p> <p>(II) Configuration can be easily modified</p>	(I) Low light efficiency due to opacity of channels of the monolith
<b>Optical fiber reactor</b>	<p>(I) High surface area and light utilization efficiency</p> <p>(II) Efficient processing capacities of the catalyst</p>	<p>(I) Maximum use of the reactor volume is not achieved</p> <p>(II) Heat build-up of fibers can lead to rapid catalyst deactivation</p>

## CHAPTER 3

### METHODOLOGY

This project studies the photocatalytic activity of doping of noble metal Ag onto the surface of the TiO<sub>2</sub> photocatalyst for the conversion of carbon dioxide, CO<sub>2</sub> to methane, CH<sub>4</sub>. The experimental design for this study includes photocatalyst materials, synthesis of TiO<sub>2</sub>, Synthesis of Ag-TiO<sub>2</sub>, Synthesis of RGO, Synthesis of RGO-Ag/TiO<sub>2</sub>, catalyst characterization and Photocatalytic Reduction of CO<sub>2</sub>. A detailed study is explained in this chapter.

#### 3.1 Material

Titanium (IV) chloride (TiCl<sub>4</sub>, 99.9%), graphite flakes (C, 99%), silver nitrate (AgNO<sub>3</sub>, 99.9%), tetrahydrofuran (THF, 99%), ethylene glycol (C<sub>2</sub>H<sub>6</sub>O, 99.8%), benzyl alcohol (C<sub>7</sub>H<sub>8</sub>O, 99.8%), potassium permanganate (KMnO<sub>4</sub>, 99.9%), sulphuric acid (H<sub>2</sub>SO<sub>4</sub>, 98%), hydrogen peroxide (H<sub>2</sub>O<sub>2</sub>, 30%), hydrogen chloride (HCl, 37%) denatured ethanol (99.7%) and deionized water.

#### 3.2 Synthesis of TiO<sub>2</sub>

Synthesis of TiO<sub>2</sub> is done by adding drop by drop of 1 ml of TiCl<sub>4</sub> in to 20ml of anhydrous benzyl alcohol while the solution is stirred. Observe the colour of the solution which will turn to red colour and then to orange colour and lastly will remain in yellowish colour with white precipitate at the bottom of the beaker. The stirring process will last for 24 hour and aged for 21 days at room temperature. Next, recover the white precipitate by centrifugation at 300rpm for 30 minutes and rinse it thoroughly with 20mL of ethanol and follow by 20ml of tetrahydrofuran (THF) for 2 times. This process is repeated for 3 times to ensure removal of Cl<sup>-</sup> anions. Lastly, dry the TiO<sub>2</sub> sample at room temperature. (Leong et al., 2015)

### 3.3 Synthesis of Ag-TiO<sub>2</sub>

0.2g of TiO<sub>2</sub> is added into the mixture of ethylene glycol which contains AgNO<sub>3</sub>. The mixture is then stirred continuously for 15 minutes under visible light. After the stirring process, the white precipitate formed is separated by centrifugation at 2000 rpm for 5 minutes. The result is then retrieved and washed it with ethanol and distilled water. This process is repeated for 2 times and lastly dries it overnight at 90°C. (Leong et al., 2015)

### 3.4 Synthesis of RGO

According to Simplified Hummers method, graphene oxide was synthesized by adding 3.0g of natural graphite powder in the mixture of 400ml of H<sub>2</sub>SO<sub>4</sub> and 18g of KMnO<sub>4</sub>. Then, stir the mixture for 3 days to complete the oxidation process. H<sub>2</sub>O<sub>2</sub> solution is then added to stop the oxidation process. Next, graphite oxide is wash with 1 M of HCl and deionized water. During the washing process, the graphite oxide underwent exfoliation to form GO gel. After that, let the GO gel to dry in vacuum at 60°C for 24 hour to obtain graphene oxide solid (GO solid). (Hummers, W.S et al., 1958)

### 3.5 Synthesis of RGO-Ag/TiO<sub>2</sub>

After getting the GO solid, dissolve 0.2g of GO solid in the deionized water under ultrasonic condition for an hour. Then add 1g of Ag/TiO<sub>2</sub> into the yellow brown solution (GO solution) and stir for 1 hour until homogenous phase appear. Next, the homogeneous solution is autoclaved at 180°C for 6 hour. This hydrothermal treatment reduce GO to RGO. After 6 hour, retrieve the result through centrifugation and wash it thoroughly through deionized water. Dry the RGO-Ag/TiO<sub>2</sub> suspension at room temperature. (Leong et al., 2015)



### 3.6 Characterization

The x-ray diffraction (XRD) patterns of the prepared photocatalyst are studied with Burker D8 Advance instrument using Cu K $\alpha$  ( $\lambda = 0.154\text{nm}$ ) radiation operating at 40 kV and 40 mA for the angle of diffraction  $2\theta$  between 10 and 80 degrees with an angular step of  $0.05^\circ \text{ s}^{-1}$ . It is used to investigate the crystalline phase composition and the grain size of the photocatalysts (Leong et al., 2015). The Figure 3.1 shows the XRD equipment photo that located in Central Lab.



Figure 3.1: X-ray Diffraction (XRD) machine model Burker D8 Advance

The physical structures of the sample are measured by field emission scanning electron microscope (FESEM) at an accelerating voltage of 20 kV (JSM-7800, Joel). Furthermore, the transmission electron microscopy (TEM) study is carried out to get the details on the element composition, crystallography and particle size distribution of the nanomaterials. Energy dispersive x-ray spectroscopy (EDX) detector is used to observe the specific structural and determine the composition of the synthesis material. These characterizations can be performed by FESEM JSM-7800F which possesses all the methods above (Leong et al., 2015). Figure 3.2 shows the FESEM machine which is used.



Figure 3.2: Field Emission Scanning Electron Microscope (FESEM) model  
JSM-7800F

UV visible spectrophotometer is used to measure the ability of the prepared photocatalysts to absorb visible light. UV visible spectrophotometer (UV-2600, Shimadzu) (Figure 3.3) which equipped with integrating sphere attachment is used. BaSO<sub>4</sub> are used as a reference to collect spectra. Metrohm Autolab (PGSTAT302N) is used to measure the transition of the photogenerated electrons in the composites. A standard three-electrode system using platinum wire as counter electrode, Ag/AgCl as reference electrode, and synthesized sample as working electrode was employed for the study. 0.1 M Na<sub>2</sub>SO<sub>4</sub> aqueous solution was used as the electrolyte solution. 500 W of tungsten–halogen lamp with a high-pass UV filter was utilized as visible light irradiation source (Leong et al., 2015).



Figure 3.3 UV Visible spectrometer model UV-2600, Shimadzu

Gas chromatography (GC) is used to identify and analysing the extracted gas samples especially methane, CH<sub>4</sub>. It is equipped with flame ionisation detector (FID) and molecular sieve 5A. It can identify specific compound in gas mixture by using respond factor. The respond factor of methane gas was evaluated by inserting different concentrations of methane standards and set at 1.34 minutes. A range of  $\pm 0.1$  to  $\pm 0.18$  minutes in the respond factor of methane was observed against time due to the nature of the column. During conditioning, the column was cleaned by let the carrier gas (He) to circulate through the injection port, column and detector at a flow rate of 25ml/min. The temperature of the detector and oven were increased to 453K and 458K. After 20 minutes, the oven was decreased to 323K with flow rate set to 5ml/min. During analysis, the base temperature use to identify methane gas of the FID detector is 523K and oven temperature is 323 for 1 minutes. Then the sample was injected into the GC. The gas was vaporized and circulated into the column and will go through FID detector which will generate signals to identify the components. Average of three readings was taken. Figure 3.4 shows the GC which located in Central Lab.



Figure 3.4: Gas Chromatography in Central Lab

### 3.7 Photocatalytic Reduction of CO<sub>2</sub>

The photocatalytic reduction of CO<sub>2</sub> is carried out in a solid gas phase photoreactor. The experiment setup is shown as the schematic diagram in Figure 3.1. The activities are evaluated under the visible light irradiation for the conversion of CO<sub>2</sub> with water vapour to CH<sub>4</sub>. A 500 W tungsten – halogen lamp with high pass UV light filter are used as the visible light source. Synthesis powdered sample, RGO-Ag/TiO<sub>2</sub> with petri dish are placed into the chamber together with a total volume of 9.8 mL highly purified CO<sub>2</sub> (99.9%) which is supplied by the mixture of CO<sub>2</sub> and water vapour. The CO<sub>2</sub> is bubbled through the water vapour into the chamber. In order to eliminate the impurities, CO<sub>2</sub> gas was ejected through the reactor at a flowrate of 300 mL min<sup>-1</sup> for 1 hour and then maintained the flowrate at 100 mL min<sup>-1</sup> for the whole experiment. The comparisons between the photocatalytic reduction of CO<sub>2</sub> and the control method are done under such conditions:

1. Absence of light irradiation but presence of photocatalyst and the flow of CO<sub>2</sub> and water vapour.
2. Absence of photocatalyst but presence of light irradiation and the flow of CO<sub>2</sub> and water vapour.
3. Absence of light irradiation but presence of photocatalyst and the flow of CO<sub>2</sub> and water vapour.
4. Under N<sub>2</sub> and water vapour flow presence of photocatalyst and the light irradiation.

The result is collected and analysed for the CH<sub>4</sub> yield using a gas chromatography system (Sim et al., 2015).

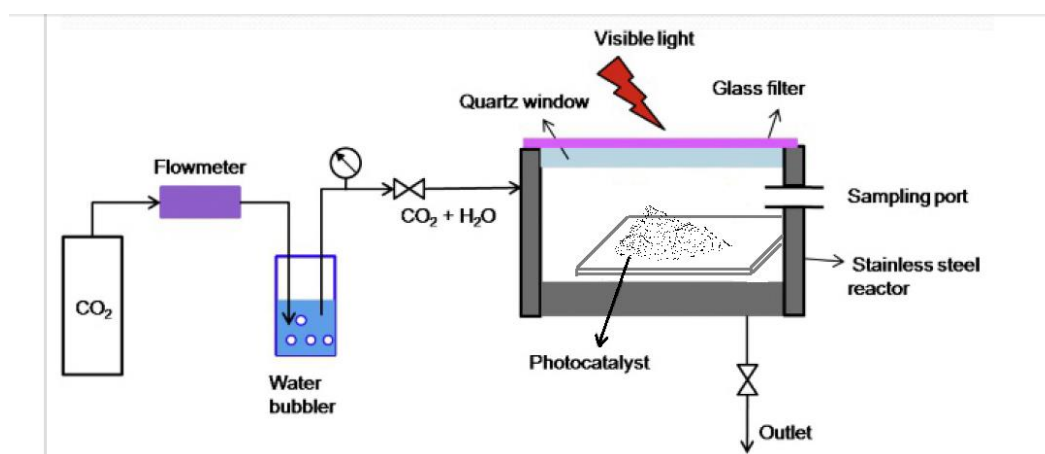


Figure 3.5: Schematic diagram of solid gas phase photoreactor

## CHAPTER 4

### RESULT AND DISCUSSION

#### 4.1 Characterization

FESEM images are successfully shown as Figure 4.1. The image Figure 4.1(a) shows the regular distribution of Ag/TiO<sub>2</sub> onto the RGO sheets and (b) shows the Ag doped onto the surface of TiO<sub>2</sub> through efficient sustainable photodeposition method, (c) and (d) shows the particle size of Ag nanoparticles (NPs) with lattice fringes spacing.

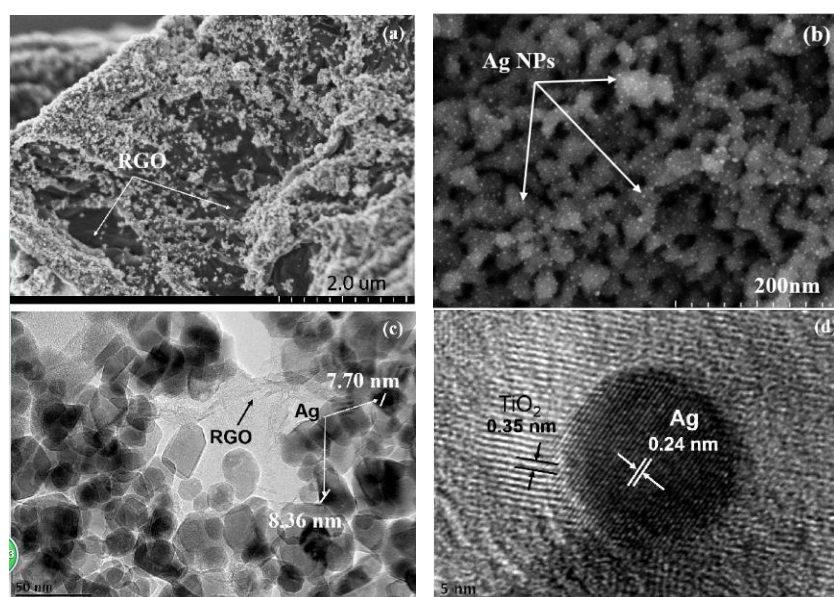


Figure 4.1 Physical surface structural of the (a) and (b) RGO-Ag/TiO<sub>2</sub> and (c) and (d) TEM images of RGO- RGO-Ag/TiO<sub>2</sub>

The structure signifies the two-dimensional transparent RGO sheets with those Ag nanoparticles that surrounded on the surface of TiO<sub>2</sub> uniformly. The morphology of the TiO<sub>2</sub> remain the same although it is warp by the impurities. The cross sectional of RGO-Ag/TiO<sub>2</sub> are clearly shown in the image with the tube length of the Ag that range between 7nm and 9nm. The synthesis photocatalyst Ag and TiO<sub>2</sub> are shown clearly by the lattice fringes recorded in TEM image of RGO-Ag/TiO<sub>2</sub> (Figure 4.1d). The lattice fringes with spacing 0.24 nm and 0.35nm are corresponding to the plane of Ag and TiO<sub>2</sub> respectively.

The characteristic of X-ray diffraction (XRD) patterns of the successfully encapsulated RGO-AgTiO<sub>2</sub> are shown as Figure 4.2. The peaks of GO, TiO<sub>2</sub>, RGO-TiO<sub>2</sub> and RGO-Ag/TiO<sub>2</sub> are shown in the graph. (Sim et al., 2015).

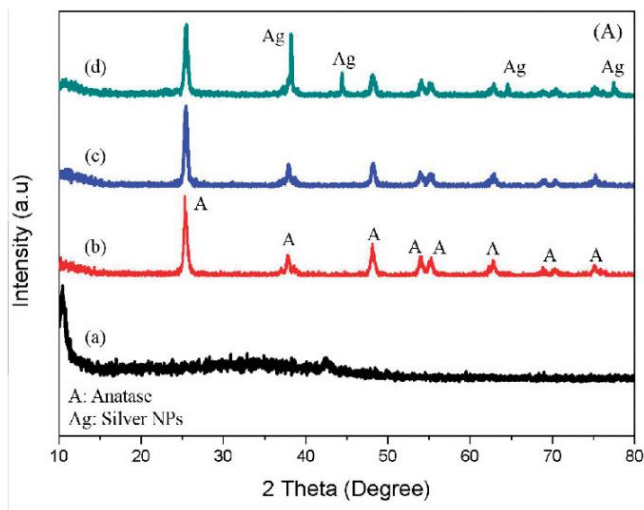


Figure 4.2: Diffraction patterns of (a) GO, (b) TiO<sub>2</sub>, (c) RGO-TiO<sub>2</sub> and (d) RGO-Ag/TiO<sub>2</sub>

The diffraction peaks are recorded at  $2\theta = 38.1^\circ$ ,  $44.3^\circ$ ,  $64.4^\circ$  and  $77.4^\circ$  which resembles to crystal phase (1 1 1), (2 0 0), (2 2 0) and (3 1 1) of Ag nanoparticles. The intense diffraction peaks confirms the synthesis of the Ag nanoparticles are very stable. A peak was seen at  $2\theta = 10.6^\circ$  (0 0 2) when GO sample signifying almost complete oxidation of nature graphite into GO by expanding the d-spacing from 0.34 to 0.93 nm. In both RGO-TiO<sub>2</sub> and RGO-Ag/TiO<sub>2</sub>, the amount of carbon species in the compound is low. Therefore, RGO did not show a visible diffraction peak. The mean crystalline size of TiO<sub>2</sub> is found to be 20.29nm which is almost the same with the pure TiO<sub>2</sub> 19.68nm. The calculation is done by using Scherrer Equation. (Equation 4.1) (Sim et al., 2015).

$$D = \frac{K\lambda}{\beta \cos\theta} \quad (\text{Eq.4.1})$$

$\beta$  is the full width half maximum (FWHM) for the  $2\theta$  peak,  $K$  is the shape factor which is 0.89 taken for the calculation,  $\lambda$  is the wavelength of X-ray which is 0.154nm and  $\theta$  is the diffraction angle. (Sim et al., 2015).

In the analysis of light absorption of the photocatalyst, UV visible spectroscopy analysis was carried out and shown as Figure 4.3(A).



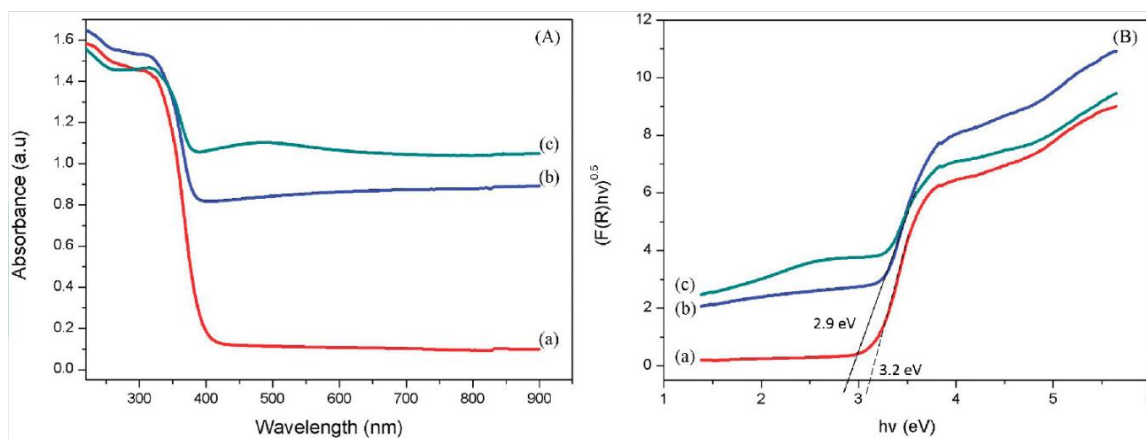


Figure 4.3: The diagram shows (A) UV visible absorption spectra (B) Calculated bandgap energies of (a) TiO<sub>2</sub>, (b) RGO-TiO<sub>2</sub> and (c) RGO-Ag/TiO<sub>2</sub>

The line move towards visible light region is clearly seen for RGO-TiO<sub>2</sub> and RGO-Ag/TiO<sub>2</sub>. This portrayed narrow bandgap energy on the RGO plane. This significant shift determines the incorporation of RGO in the photocatalyst through Ti-O-C bond. The improvement in the visible light region at ~460nm can be seen after incorporation of Ag nanoparticles into RGO-Ag/TiO<sub>2</sub>. The doping of Ag nanoparticles on the surface of photocatalyst, TiO<sub>2</sub> leads to visible light absorption. Figure 4.3(B) shows the calculated bandgap energy for the prepared photocatalysts. After the incorporation of RGO, the bandgap energy of TiO<sub>2</sub> was tuned to 2.9eV. The reduction of bandgap is caused by the Ti-O-C bond. The electron surface of TiO<sub>2</sub> is bonded with unpaired  $\pi$ -electrons and shift the electron to the valance band edge. The observed phenomenon boost the RGO-Ag/TiO<sub>2</sub> with a notable visible light performance. (Sim et al., 2015).

## 4.2 Photocatalytic Reduction of CO<sub>2</sub>

There is a series of control experiments were carried out to proof that the mainly yield of methane, CH<sub>4</sub> is come from photocatalytic reduction of CO<sub>2</sub>. The control experiments are:

1. Absence of light irradiation but presence of photocatalyst and the flow of CO<sub>2</sub> and water vapour.
2. Absence of photocatalyst but presence of light irradiation and the flow of CO<sub>2</sub> and water vapour.

3. Absence of light irradiation but presence of photocatalyst and the flow of CO<sub>2</sub> and water vapour.

4. Under N<sub>2</sub> and water vapour flow presence of photocatalyst and the light irradiation.

Figure 4.4 indicates the insignificant CH<sub>4</sub> yield presence in these control tests. This reveals that most of the CH<sub>4</sub> is produce by the present of photocatalyst, CO<sub>2</sub>, water vapour and light irradiance. The graph in Figure 4.4 shows that the total CH<sub>4</sub> yield increase in order from anatase TiO<sub>2</sub>, ( $5.67 \mu\text{mol m}^{-2}$ ) < RGO-TiO<sub>2</sub> ( $6.89 \mu\text{mol m}^{-2}$ ) < Ag-TiO<sub>2</sub>( $9.03 \mu\text{mol m}^{-2}$ ) < RGO-Ag/TiO<sub>2</sub>( $10.965.67 \mu\text{mol m}^{-2}$ ).

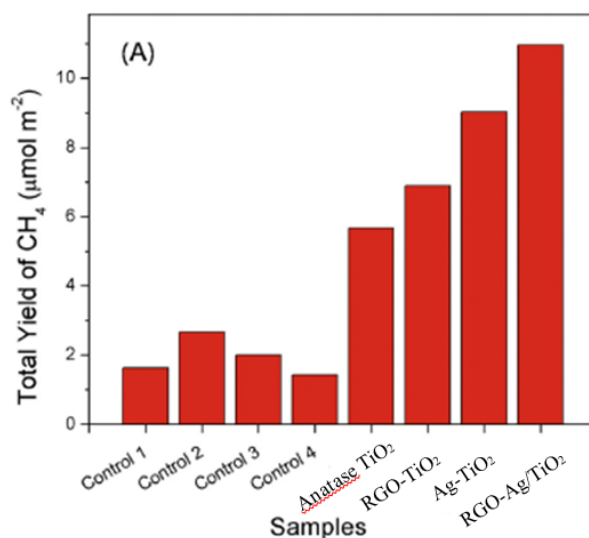


Figure 4.4: The total yield of CH<sub>4</sub> over Control 1, Control 2, Control 3, Control 4, Anatase TiO<sub>2</sub>, RGO-TiO<sub>2</sub>, Ag-TiO<sub>2</sub> and RGO-Ag/TiO<sub>2</sub>.



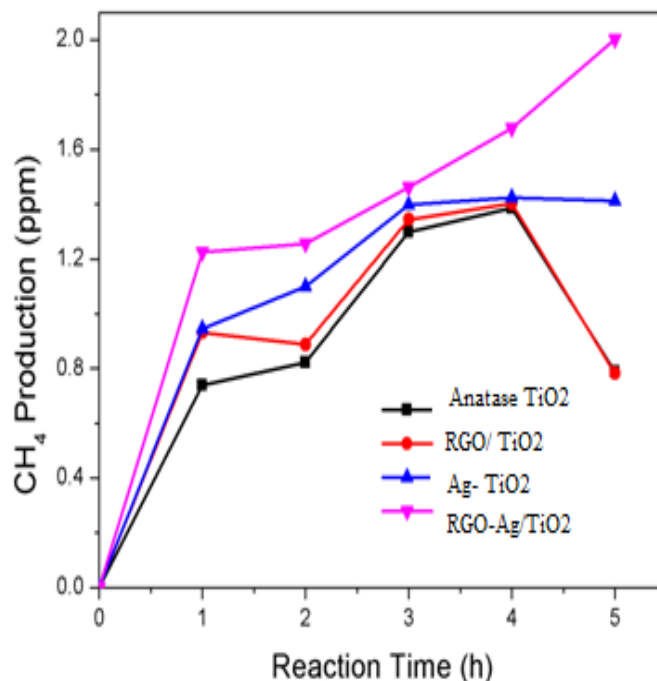


Figure 4.5: Time dependence on the production rate of CH<sub>4</sub>

Figure 4.5 reveals that the minimal CH<sub>4</sub> production rate is obtained by anatase TiO<sub>2</sub> which has a maximum yield of  $1.28 \mu\text{mol m}^{-2}\text{h}^{-1}$ . It obviously shows that pure TiO<sub>2</sub> are not sensitive to absorb visible light due to its huge bandgap. The combination of RGO/TiO<sub>2</sub> enhance the moving electron from the anatase TiO<sub>2</sub> to RGO, hence the production of the CH<sub>4</sub> increased to  $1.60 \mu\text{mol m}^{-2}\text{h}^{-1}$ . The maximum production rate of CH<sub>4</sub> is RGO-Ag/TiO<sub>2</sub> which is  $2.88 \mu\text{mol m}^{-2}\text{h}^{-1}$ . The photoreduction efficiency increased from anatase TiO<sub>2</sub> to RGO-TiO<sub>2</sub> to Ag/TiO<sub>2</sub> and lastly RGO-Ag/TiO<sub>2</sub>.

RGO-Ag/TiO<sub>2</sub> made an increase in total yield of CH<sub>4</sub> which comparable with anatase TiO<sub>2</sub> and RGO-TiO<sub>2</sub>. Ag nanoparticles have the unique characteristic of negative work function (4.26eV) which can absorb the photogenerated electron of TiO<sub>2</sub>. As the Ag nanoparticles and the RGO combined, the electron will be absorbed from the Ag nanoparticles to surface of RGO. Moreover, the LSPR phenomenon was excited by the adoption of noble metal under presence of visible light. The presence of visible light triggered Ag nanoparticles surface plasmon and cause generation of high concentration electron on its surface. The occurrence of electron collision excited the electron movement from valance band (VB) to conduction band (CB) of TiO<sub>2</sub>. Then, the contacted RGO surface quickly transfers those electrons through  $\pi$ - conjugation structure. Ag nanoparticles mainly reduces the conduction electron bandgap (CB),

makes the electrons easier to jump from the VB to the CB of TiO<sub>2</sub>. This effective movement of electrons from Ag to RGO surface prolongs the life span of the charge carriers. As the electron was excited from VB to CB, there is an occurrence of holes at VB.

Furthermore, the excess formation of the electron through Ag will also reacts with the surface absorb oxygen to form superoxide anion radical ( $O_2^-$ ) whereas the holes form active radicals (OH) by reacting with water molecules ( $H_2O$ ). The OH radicals triggered suppression of electron-holes recombination. This default was conquered by doping Ag/TiO<sub>2</sub> onto RGO sheets surface to prolong the lifetime of electron-hole pairs. The electrons trapped at RGO will reduce the CO<sub>2</sub> to CO. Then produced CO then combine with hydrogen ion through reduction process to yield CH<sub>4</sub>. (Figure 4.6) (Sim et al., 2015).

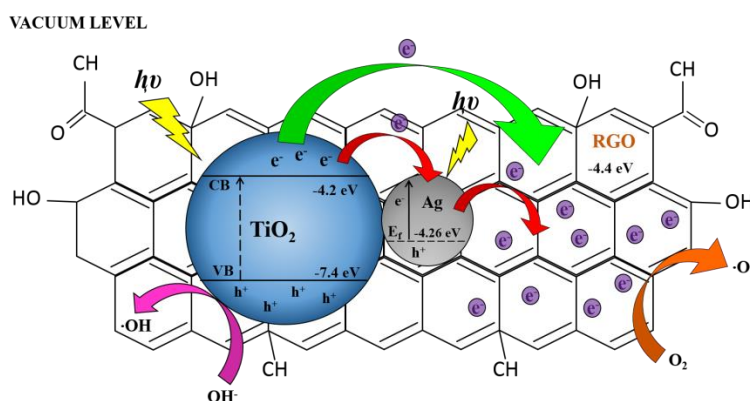


Figure 4.6: Excitation mechanism of RGO-Ag/TiO<sub>2</sub> photocatalyst under visible light irradiation.

### 4.3 Project Management

#### 4.3.1 Budget and Cost Analyses

**Table 4.1:** List of Cost Chemicals

	<b>Chemicals</b>	<b>Quantities</b>	<b>Cost (RM)</b>	<b>Total Cost (RM)</b>
1.	TiCl <sub>4</sub> (99.9%)	1	317	317
2.	C (99%)	1	2,221	2,221
3.	AgNO <sub>3</sub> (99.9%)	1	1,132	1,132
4.	C <sub>4</sub> H <sub>8</sub> O (99.9%)	1	783	783
5.	C <sub>2</sub> H <sub>6</sub> O <sub>2</sub> (99.8%)	1	726	726
6.	C <sub>7</sub> H <sub>8</sub> O (99.8%)	1	905	905
7.	KMnO <sub>4</sub> (99.9%)	1	109	109
8.	H <sub>2</sub> SO <sub>4</sub> (98%)	1	138	138
9.	H <sub>2</sub> O <sub>2</sub> (30%)	1	145	145
10.	HCl (37%)	1	152	152
11.	C <sub>2</sub> H <sub>6</sub> O (95%)	1	138	138
	<b>TOTAL (including GST)</b>			7,171.96

**Table 4.2:** List of Cost Materials of Reactor

<b>No.</b>	<b>Materials</b>	<b>Quantities</b>	<b>Cost (RM)</b>	<b>Total Cost (RM)</b>
1.	Dwyer Rate Flowmeter	2	119.00	238.00
2.	Pressure Gauge	1	180.00	180.00
3.	Stainless Steel Ball Valve	2	30.00	60.00
4.	Push In Fitting 1/8-6	10	5.41	54.10
5.	Push In Fitting 1/4-6	3	6.25	18.75
6.	Elbow Push In Fitting 1/4-6	1	15.00	15.00
7.	Push In Tee Fitting 1/4-6	1	13.25	13.25
8.	U-clip	4	3.00	12.00
9.	Brass Reducing Bush 1/4x1/8	1	4.24	4.24
10.	Brass Reducing Bush 3/8x1/4	3	5.30	15.90
11.	Black Tubing	5	3.20	16.00
12.	O-Ring 11	4	0.35	1.40
13.	O-Ring 30	1	0.75	0.75
14.	Cable Gland 3.5-6	6	1.10	6.60
15.	Labotary Glass Bottle 250ml	1	15.00	15.00
16.	Aluminium Sheet	1	200.00	200.00
17.	Mild Steel Square Tube	1	200.00	200.00
<b>TOTAL (including GST)</b>				1,051

### 4.3.2 Workflow

**Table 4.3:** Project Workflow

ACTIVITY	Week													
	1	2	3	4	5	6	7	8	9	10	11	12	13	14
Short briefing from Dr Che Ku														
Discussion on the project about the photocatalyst experiment and photoreactor														
Describe all the methodology <ul style="list-style-type: none"> <li>i. Materials</li> <li>ii. Synthesis of TiO<sub>2</sub></li> <li>iii. Synthesis of Ag-TiO<sub>2</sub></li> <li>iv. Synthesis of RGO</li> <li>v. Synthesis of RGO-Ag/TiO<sub>2</sub></li> <li>vi. Characterization</li> <li>vii. Photocatalytic Reduction of CO<sub>2</sub></li> </ul>														
Preparation the application form of workshop, training chemical hazardous and risk assessment														
Start the photocatalyst experiment														
Characterization														
Poster preparation														
Thesis write-up														
Submission of first draft thesis report, extended abstract and logbook														
Mock presentation of project														
Improvisation of the final individual thesis report														
Submission of Presentation Approval Form and poster														
Submission of the final individual thesis report, extended abstract, peer evaluation form and general handling form														
Presentation of the project														

## CHAPTER 5

### CONCLUSION AND RECOMMENDATION

#### 5.1 Conclusion

Global warming is very crucial problem that occurs nowadays. Carbon dioxide, CO<sub>2</sub> emissions are one of the main causes of global warming. Our project entitles “Development of Photocatalyst for CO<sub>2</sub> Conversion to Hydrocarbon Fuel” mainly find a solution to tackle the excess CO<sub>2</sub> in our atmosphere. Among all semiconductors, Titanium dioxide, TiO<sub>2</sub> has a valuable properties. It can be use on reducing CO<sub>2</sub> through simple method. However, the limitation of TiO<sub>2</sub> is due to its large band gap. Furthermore, TiO<sub>2</sub> will only respond under ultraviolet light which is 2% to 5% sunlight. After concluding, it is important to carry out investigation on the photoconversion of CO<sub>2</sub> by using modified TiO<sub>2</sub> to enhance the conversion of CO<sub>2</sub> to useful hydrocarbon fuel.

The synthesis of photocatalyst, RGO-Ag/TiO<sub>2</sub> was successfully done in our project through a simple method. The photocatalyst TiO<sub>2</sub> is doped with noble metal Silver, Ag and then been warped onto the surface of RGO. The Ag can enhance the electron transfer from the TiO<sub>2</sub> to RGO and increase the rate of conversion of CO<sub>2</sub> to methane, CH<sub>4</sub>. The Ag nanoparticle supported the composited through energetic LSPR phenomenon which increase the production of hydroxyl radical and delayed the electron and holes. It is a significant photocatalyst which can reduce CO<sub>2</sub> under presence of light irradiance. Therefore, the composition of RGO-Ag/TiO<sub>2</sub> provides an opportunity to simply describe the methodology to tackle the causes of global warming.

A series of characterization was carried out to determine the acceptance of visible light on the composite RGO-Ag/TiO<sub>2</sub>. Field emission scanning electron microscope, FESEM is used to determine the physical surface structure of the photocatalyst. The morphology does not change as the doping of noble metal occurs. Transmission electron microscopy, TEM study the details on the element composition, crystallography and particle size distribution of the nanomaterials. While, dispersive x-ray spectroscopy, EDX detector is used to observe the specific structural and determine the composition of the synthesis material. X-ray diffraction, XRD analysed the crystalline phase composition and the grain size of the photocatalysts. The peak of

diffraction shows the phase structure of the Ag which is  $77.4^\circ$  for RGO-Ag/TiO<sub>2</sub>. UV visible spectrometer use to determine the absorption of visible light of the photocatalyst. RGO-Ag/TiO<sub>2</sub> has the highest light absorption value. Gas chromatography, GC is use at last to identify the presence and the concentration of methane gas. The highest concentration of the CH<sub>4</sub> is produced by photocatalyst RGO-Ag/TiO<sub>2</sub>.

## 5.2 Recommendation

All in all, this project is focus on the synthesis and the characterization of photocatalyst which doped by noble metal for the reduction of CO<sub>2</sub> under visible light. The limitation of economic and technical must be overcome if this alternative energy needs to be commercialised. The expenditure for the feedstock such as CO<sub>2</sub>, H<sub>2</sub>O and solar energy will controls the fuel price. The characteristic of the CO<sub>2</sub> is also a concern to produce significant CH<sub>4</sub>. The cost will also need to include the overall cost of the capital such as equipment for example solar collectors. Furthermore, the scale up photoreactor needs to be reconfigured due to get the most efficiency of CO<sub>2</sub> reduction. Therefore, the next phase on the development of photocatalyst RGO-Ag/TiO<sub>2</sub> should be focus on the testing of performance and processing capacity in a given reactor volume. Besides, the understanding of engineering aspects of CO<sub>2</sub> reduction is also needed an efficient reactor. Therefore, the efficiency on designing the photoreactor is encouraged to enhance the conversion efficiency. Besides, further works on different composition of flue gas streams can be used as a feedstock for CO<sub>2</sub> reduction. The impurities of the concentration of CO<sub>2</sub> can be determine and used to achieve the best concentration of CO<sub>2</sub>.

## REFERENCES

- Albiter, E., Valenzuela, M. A., Alfaro, S., Valverde-Aguilar, G., & Martínez-Pallares, F. M. (2015). Photocatalytic deposition of Ag nanoparticles on TiO<sub>2</sub>: Metal precursor effect on the structural and photoactivity properties. *Journal of Saudi Chemical Society*, 19(5), 563–573. <http://doi.org/10.1016/j.jscs.2015.05.009>
- Anpo, M., Yamashita, H., Ichihashi, Y., & Ehara, S. (1995). Photocatalytic reduction of CO with H<sub>2</sub>O on various titanium oxide catalysts. *Journal of Electroanalytical Chemistry*, 396, 21–26. Retrieved from [http://reichling.physik.uos.de/download\\_paper.php?paper=JElectroanalChem396p21\(1995\)\\_Anpo.pdf](http://reichling.physik.uos.de/download_paper.php?paper=JElectroanalChem396p21(1995)_Anpo.pdf)
- Enachi, M., Guix, M., Braniste, T., Postolache, V., Ciobanu, V., Ursaki, V., ... Tiginyanu, I. (2015). Photocatalytic properties of TiO<sub>2</sub> nanotubes doped with Ag, Au and Pt or covered by Ag, Au and Pt nanodots. *Surface Engineering and Applied Electrochemistry*, 51(1), 3–8. <https://doi.org/10.3103/S1068375515010044>
- Feng, S., Wang, M., Zhou, Y., Li, P., Tu, W., & Zou, Z. (2015). Double-shelled plasmonic Ag-TiO<sub>2</sub> hollow spheres toward visible light-active photocatalytic conversion of CO<sub>2</sub> into solar fuel. *APL Materials*, 3(10). <https://doi.org/10.1063/1.4930043>
- Hummers, W. S., & Offeman, R. E. (1958). Preparation of Graphitic Oxide. *Journal of the American Chemical Society*, 80(6), 1339–1339. <https://doi.org/10.1021/ja01539a017>
- Huang, F., Yan, A., & Zhao, H. (n.d.). Influences of Doping on Photocatalytic Properties of TiO<sub>2</sub> Photocatalyst. <https://doi.org/10.5772/63234>
- Jiang, Z., Xiao, T., Kuznetsov, V. L., & Edwards, P. P. (2010). Turning carbon dioxide into fuel. *Phil. Trans. R. Soc. A*, 368, 3343–3364. <https://doi.org/10.1098/rsta.2010.0119>
- Kumar, R., Rashid, J., & Barakat, M. A. (2015). Zero valent Ag deposited TiO<sub>2</sub> for the efficient photocatalysis of methylene blue under UV-C light irradiation. *Colloids and Interface Science Communications*, 5, 1–4. <https://doi.org/10.1016/j.colcom.2015.05.001>
- Leong, K. H., Sim, L. C., Bahnemann, D., Jang, M., Ibrahim, S., & Saravanan, P. (2015). Reduced graphene oxide and Ag wrapped TiO<sub>2</sub> photocatalyst for enhanced visible light photocatalysis. *APL Materials*, 3(10), 104503. <http://doi.org/10.1063/1.4926454>



- Li, K., An, X., Park, K. H., Khraisheh, M., & Tang, J. (2014). A critical review of CO<sub>2</sub> photoconversion: Catalysts and reactors. *Catalysis Today*, 224, 3–12. <https://doi.org/10.1016/j.cattod.2013.12.006>
- Ola, O., & Maroto-Valer, M. M. (2015). Review of material design and reactor engineering on TiO<sub>2</sub> photocatalysis for CO<sub>2</sub> reduction. *Journal of Photochemistry and Photobiology C: Photochemistry Reviews*, 24, 16–42. <https://doi.org/10.1016/j.jphotochemrev.2015.06.001>
- Petryayeva, E., & Krull, U. J. (2011). Localized surface plasmon resonance: Nanostructures, bioassays and biosensing—A review. *Analytica Chimica Acta*, 706(1), 8–24. <https://doi.org/10.1016/j.aca.2011.08.020>
- Piumetti, M., Fino, D., & Russo, N. (2014). Photocatalytic Reduction of CO<sub>2</sub> into Fuels: A Short Review. *Journal of Advanced Catalysis Science and Technology*, 1, 16–25. Retrieved from [http://cosmoscholars.com/images/JACST-EBMs/JACST-V1-N2/JACST\\_V1N2A3-Russo.pdf](http://cosmoscholars.com/images/JACST-EBMs/JACST-V1-N2/JACST_V1N2A3-Russo.pdf)
- Sim, L. C., Leong, K. H., Saravanan, P., & Ibrahim, S. (2015). Rapid thermal reduced graphene oxide/Pt-TiO<sub>2</sub> nanotube arrays for enhanced visible-light-driven photocatalytic reduction of CO<sub>2</sub>. *Applied Surface Science*, 358, 122–129. <http://doi.org/10.1016/j.apsusc.2015.08.065>
- Sim, L. C., Ng, K. W., Ibrahim, S., & Saravanan, P. (2013). Preparation of Improved p-n Junction NiO / TiO<sub>2</sub> Nanotubes for Solar-Energy-Driven Light Photocatalysis. *International Journal of Photoenergy*, 2013, 1–10. <https://doi.org/10.1155/2013/659013>
- Sim, L. C., Ng, K. W., Ibrahim, S., & Saravanan, P. (2014). Synthesis, Features and Solar-Light-Driven Photocatalytic Activity of TiO<sub>2</sub> Nanotube Arrays Loaded with SnO<sub>2</sub>. *Journal of Nanoscience and Nanotechnology*, 14(9), 7001–7009. <https://doi.org/10.1166/jnn.2014.8931>
- Izumi, Y. (2013). Recent advances in the photocatalytic conversion of carbon dioxide to fuels with water and/or hydrogen using solar energy and beyond. *Coordination Chemistry Reviews*, 257(1), 171–186. <https://doi.org/10.1016/j.ccr.2012.04.018>
- Tang, J., Guo, Z., & Jamali, A. (n.d.). CO<sub>2</sub> capture and photocatalytic conversion to a renewable fuel on nanostructured catalysts. Retrieved from <http://www.ucl.ac.uk/btg/FeedbackReports/BtGReportTang1.pdf>
- CO<sub>2</sub> - the major cause of global warming | Time for change. (n.d.). Retrieved May 11, 2017, from <http://timeforchange.org/CO2-cause-of-global-warming>

## APPENDICES



Figure 1: This is our photocatalyst RGO-Ag/TiO<sub>2</sub>

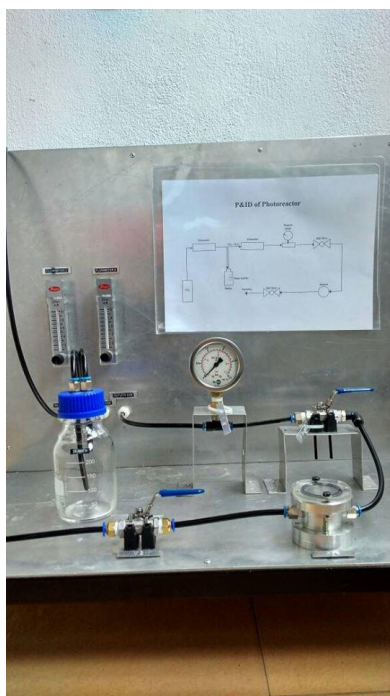


Figure 2: This is the real prototype of photocatalyst reactor